

# A Multiple Electrode Scheme for Optimal Non-Invasive Electrical Stimulation

Jacek P. Dmochowski\*, Marom Bikson\*, Abhishek Datta\*, Yuzhuo Su<sup>†</sup>, and Lucas C. Parra\*

\*Department of Biomedical Engineering  
City College of New York  
New York, NY 10031

Email: [jdmochowski@ccny.cuny.edu](mailto:jdmochowski@ccny.cuny.edu)

<sup>†</sup>Neuromatters LLC  
New York, NY 10005

**Abstract**—Transcranial electrical stimulation involves the delivery of weak electrical currents to the brain via scalp electrodes to elicit neuromodulatory effects. The current is conventionally passed through two large electrodes resulting in diffused electric fields. In this paper, we propose a novel paradigm in which multiple small electrodes with independent current controls are systematically optimized to yield targeted and effective stimulation under safety constraints. We employ the finite element method, in conjunction with a magnetic resonance imagery based model of the human head, to formulate a linear system relating the applied scalp current to the resulting electric field. Optimization techniques are then applied to derive stimulation parameters which maximize either intensity or focality at the target location. Results demonstrate that the optimal electrode configuration is strongly dependent on both the desired field orientation and the optimization criterion. The proposed scheme yields improvements of 98% in target intensity and 80% in focality compared to the conventional two-electrode montage. Additionally, the presented framework effectively optimizes electrode placement in the classical bipolar configuration, which is useful if only a single channel current source is available. Consequently, the proposed scheme promises to deliver increased efficacy and improved patient safety to clinical settings in which the target site is identified by a clinician.

## I. INTRODUCTION

Transcranial direct current stimulation (tDCS) is an emerging neurotechnology involving the application of small direct currents to the surface of the scalp to elicit modulation of neural activity [1]. It is currently being investigated as a therapeutic tool for a wide array of neurological conditions, including major depression [2], epilepsy [3], Parkinson’s disease [4], and motor and speech rehabilitation after stroke [5], [6]. Moreover, tDCS has been shown to improve cognitive function, specifically memory, in healthy subjects [7], [8]. A basic tDCS “kit” consists of a pair of electrodes, a battery, and a simple circuit capable of injecting a controlled current intensity at the stimulating electrode while drawing an equivalent return current at the reference electrode. The procedure is inexpensive, well-tolerated, and flexible, with effects lasting well beyond the duration of the stimulation [1].

Two factors hindering the rational clinical deployment of tDCS are the limited stimulation intensities and difficulty in precisely focusing the stimulating electric fields. A significant fraction of the injected current is shunted through the scalp,

thus bypassing the brain and limiting the intensity of the field in the target region. Additionally, a lack of focal stimulation results from the diffusion of the current through the highly conductive cerebrospinal fluid (CSF). In this paper, we employ precise forward-models of current flow which are leveraged to achieve desired electric field intensities at target brain regions while sparing other areas. We consider the international 10/10 electrode placement system with 64 electrodes and optimize the current applied at each electrode such that the resulting electric field is as close as possible, in a least squares sense, to a desired field. The large number of electrode locations considered does not mean that all electrodes will be energized; rather, the locations should be viewed as candidates to place a smaller number of physical electrodes.

A critical factor that will be considered is the maximum total current delivered to the subject. A widely accepted standard for safety and comfort of weak-current electrical stimulation is to limit the total current delivered to 2 mA. As will be shown, this constraint limits the degrees of freedom and thus the achievable intensity and focality. Consequently, we also report unconstrained results to determine the upper-bound on transcranial focality. Additionally, these results may be relevant for high-intensity protocols which are routinely used clinically, namely transcutaneous electrical stimulation and electroconvulsive therapy. In general, while the results presented pertain specifically to tDCS, the proposed framework is applicable to all noninvasive electrical stimulation modalities.

The literature on optimizing electrical stimulation is scarce; more surprising is the lack of acknowledgment of the focality problem belonging to the class of beamforming techniques. The nature of the current flow induced by tDCS has been studied in [9]–[11]. In [12], the authors search the electrode position space to locate a bipolar configuration yielding the largest current flow at the target under a total current constraint. The effect of white matter anisotropy on focality is treated in [13]. The idea of utilizing multiple electrodes for optimizing tDCS has been proposed in abstract form [14].

## II. PROBLEM FORMULATION

Consider a heterogeneous volume as in Figure 1 with a scalar conductivity field  $\sigma$  (we ignore anisotropy and assume

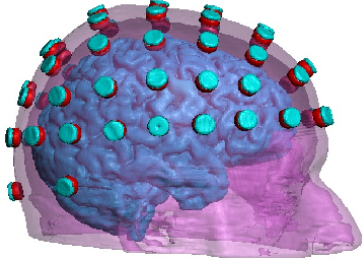


Fig. 1. Head model segmented into various tissue categories based on T1-weighted MRI image. 64 electrodes are placed according to the international 10/10 system. Red indicates the gel between electrode (magenta) and scalp (purple). Brain shown in blue.

isotropic conductivities as listed in Table I). Because the tissue has no net current sources or sinks, the current density  $\mathbf{J}$ , inside the tissue has zero divergence:  $\nabla \cdot \mathbf{J} = 0$  ( $\nabla = [\frac{\partial}{\partial x}, \frac{\partial}{\partial y}, \frac{\partial}{\partial z}]$  is the gradient operator.) Thus, when applying currents through electrodes to the boundary of this volume, the resulting potential distribution  $V$  in the volume can be found as the solution to Laplace’s equation [15]:

$$\nabla \cdot \mathbf{J} = \nabla \cdot (\sigma \mathbf{E}) = -\nabla \cdot (\sigma \nabla V) = 0. \quad (1)$$

The solution is unique given that the electric field,  $\mathbf{E}$  (or equivalently, current density,  $\mathbf{J}$ ) is specified at all locations on the outer boundary, and assuming continuity of electric potential and current density at tissue boundaries. In general, the solution does not have a closed-form. However, a numerical approximation may be found by discretizing the volume into a set of finite elements, each with a single conductivity value, and solving (1) using finite element method (FEM) [16], [17].

tissue	conductivity (S/m)
brain	0.2
skull	0.01
CSF	1.65
scalp	0.465
muscle	0.334
air	$1 \times 10^{-15}$
electrode	$5.9 \times 10^7$
gel	0.3

TABLE I  
CONDUCTIVITY VALUES  $\sigma$  ASSIGNED TO MODEL COMPONENTS.

Consider a setup in which  $M$  stimulating electrodes and an additional reference electrode are available (as there are 64 total electrodes in the 10/10 configuration,  $M = 63$ ). Let  $\mathcal{B}_m$ ,  $m = 1, \dots, M$ , denote the  $m$ th set of boundary conditions:  $\mathcal{B}_m$  consists of unit current density applied to electrode  $m$ , a negative unit current density at the reference electrode, and zero current density perpendicular to the scalp at all other boundary locations. The FEM solution yields, for each  $\mathcal{B}_m$ , the effective resistivity  $\mathbf{a}_m \in \mathbb{R}^3$  relating the current flowing into (out of) the stimulating (reference) electrodes to the electric field  $\mathbf{e}_m \in \mathbb{R}^3$  throughout the volume<sup>1</sup>:

$$\mathbf{e}_m(\mathbf{r}_n) = s_m \mathbf{a}_m(\mathbf{r}_n), \quad (2)$$

<sup>1</sup>We abandon classical physics notation in favor of linear algebraic conventions, with vectors denoted by lower-case bold font and matrices with upper-case bold.

where  $\mathbf{e}_m(\mathbf{r}_n)$  denotes the electric field vector at FEM node  $\mathbf{r}_n \in \mathbb{R}^3$ ,  $n = 1, \dots, N$ , induced by stimulation of electrode  $m$ , and  $s_m$  is the applied current density magnitude (for simplicity, we assume that the direction of the applied current is fixed, such as normal to the electrode surface, and work with scalar magnitudes  $s_m$ ). If we now simultaneously stimulate all electrodes such that the current density magnitude at electrode  $m$  is given by  $s_m$ , then the linearity of Laplace’s equation dictates that the net electric field at location  $\mathbf{r}_n$  is given by:

$$\mathbf{e}(\mathbf{r}_n) = \sum_{m=1}^M \mathbf{e}_m(\mathbf{r}_n) = \sum_{m=1}^M s_m \mathbf{a}_m(\mathbf{r}_n). \quad (3)$$

Stacking column-wise across the discrete location space and re-writing in matrix form results in:

$$\mathbf{e} = \mathbf{A} \mathbf{s}, \quad (4)$$

where

$$\mathbf{A} = \begin{bmatrix} \mathbf{a}_1(\mathbf{r}_1) & \mathbf{a}_2(\mathbf{r}_1) & \cdots & \mathbf{a}_M(\mathbf{r}_1) \\ \mathbf{a}_1(\mathbf{r}_2) & \mathbf{a}_2(\mathbf{r}_2) & \cdots & \mathbf{a}_M(\mathbf{r}_2) \\ \vdots & \vdots & \ddots & \vdots \\ \mathbf{a}_1(\mathbf{r}_N) & \mathbf{a}_2(\mathbf{r}_N) & \cdots & \mathbf{a}_M(\mathbf{r}_N) \end{bmatrix},$$

$$\mathbf{e} = \begin{bmatrix} \mathbf{e}(\mathbf{r}_1) \\ \mathbf{e}(\mathbf{r}_2) \\ \vdots \\ \mathbf{e}(\mathbf{r}_N) \end{bmatrix}, \quad \mathbf{s} = \begin{bmatrix} s_1 \\ s_2 \\ \vdots \\ s_M \end{bmatrix}.$$

The net electric field is a linear combination of the individual electric fields yielded by each bipolar configuration as computed by the FEM solver. It is clear that the nature of the field is intimately related to the individual current densities  $s_m$ . This fact allows us to tune these current densities such that the resulting field is optimal with respect to a specified measure. With  $M$  stimulating electrodes, we have  $M$  degrees of freedom at our disposal. Note that assuming uniform electrodes across the scalp, the current density at the reference electrode is given by  $-\sum_m s_m$ . The problem of choosing the coefficients  $s_m$  to shape the induced field is analogous to the “beamforming” problem in array signal processing [18]. The columns of  $\mathbf{A}$  represent linearly independent “paths” which may be intelligently combined to yield a maximally focal (or intense) net electric field at the target. Below, we propose several optimization schemes suitable for optimizing non-invasive electrical stimulation modalities.

### III. OPTIMIZATION SCHEMES

#### A. Optimizing for Focality

In the beamforming literature, a common scheme is to enforce a hard linear constraint (e.g., enforce a desired gain for a given direction) while utilizing the remaining degrees of freedom to minimize the total power. Analogously, here we want to achieve a specified electric field at a single node while minimizing the electric field elsewhere. To that end, denote the desired electric field at the target node by  $\mathbf{e}_o \in \mathbb{R}^3$ : a sensible choice for the direction specified by  $\mathbf{e}_o$  is radial

or tangential to the skull surface, particularly in the case of cortical stimulation; its magnitude conveys the desired target intensity. From all current distributions  $\mathbf{s}$  that satisfy the hard constraint, the linearly constrained minimum variance (LCMV) procedure selects the one with the lowest overall electric field power  $\|\mathbf{A}\mathbf{s}\|^2$  across the volume:

$$\mathbf{s}_{\text{lcmv}} = \arg \min_{\mathbf{s}} \|\mathbf{A}\mathbf{s}\|^2 \text{ subject to } \mathbf{C}\mathbf{s} = \mathbf{e}_o, \quad (5)$$

where

$$\mathbf{C} = [ \mathbf{a}_1(\mathbf{r}_{n_o}) \quad \mathbf{a}_2(\mathbf{r}_{n_o}) \quad \cdots \quad \mathbf{a}_M(\mathbf{r}_{n_o}) ], \quad (6)$$

and  $n_o$  is the index of the target node. The solution to (5) follows from the method of Lagrange multipliers as:

$$\mathbf{s}_{\text{lcmv}} = (\mathbf{A}^T \mathbf{A})^{-1} \mathbf{C}^T [ \mathbf{C} (\mathbf{A}^T \mathbf{A})^{-1} \mathbf{C}^T ]^{-1} \mathbf{e}_o. \quad (7)$$

Unfortunately, the solution of (7) is free to take values outside of the allowable range for safety: in conventional bipolar tDCS, the amount of current injected into the stimulating electrode is constrained to  $I_{\text{max}}$ , with  $I_{\text{max}}$  typically equalling 2 mA. Denoting the (fixed) electrode area by  $A$ , we analogously define  $s_{\text{max}} = I_{\text{max}}/A$ . It is not straightforward to extend this safety constraint to multiple electrode stimulation. The safest approach is to limit the sum of all positive currents to  $I_{\text{max}}$ . Since the sum of positive currents equals the sum of negative currents, this is equivalent to limiting the sum of absolute values of all currents to  $2I_{\text{max}}$ . Thus, the safety constrained LCMV problem follows as:

$$\begin{aligned} \mathbf{s}_{\text{lcmv-con}} = \arg \min_{\mathbf{s}} \|\mathbf{A}\mathbf{s}\|^2 \text{ subject to:} \\ \mathbf{C}\mathbf{s} = \mathbf{e}_o \text{ and } \sum_m |s_m| + \left| \sum_m s_m \right| \leq 2s_{\text{max}}, \end{aligned} \quad (8)$$

for which an iterative solution may be found using conventional numerical methods (see section V).

Note that  $\sum_m |s_m| = \|\mathbf{s}\|_1$  is by definition the  $\ell_1$  norm of the current density vector (the term  $|\sum_m s_m|$  accounts for the current through the reference electrode). Optimization with an  $\ell_1$  norm constraint is popular due to the fact that the resulting solutions often exhibit sparseness. Thus, by limiting the maximum total current we are not only satisfying a sensible safety constraint but also encouraging solutions in which a majority of the current is being guided through just a few electrodes. This has the advantage of potentially requiring fewer independent current-control channels.

The above safety constraint is guided by the notion that the effect of the injected current is globally additive. However, this may not be an accurate representation of the safety limitations of electrical stimulation as some electrode configurations may act only locally; for example, bipolar electrodes on one side of the head will not affect brain tissue on the other side of the head. In this case, a more local safety constraint guided by skin reaction and sensation levels directly under each electrode may be more appropriate. In those cases, it may be suitable to relax the safety constraint on  $\|\mathbf{s}\|_1$  and rather limit the absolute value of the current at each individual electrode. Such a procedure

may be especially valid if the set of stimulating electrodes are a considerable distance apart.

We thus also formulate the individually  $\ell_1$  constrained LCMV problem as:

$$\mathbf{s}_{\text{lcmv-ind}} = \arg \min_{\mathbf{s}} \|\mathbf{A}\mathbf{s}\|^2 \text{ subject to:}$$

$$\mathbf{C}\mathbf{s} = \mathbf{e}_o \text{ and } |s_m| \leq s_{\text{max}}, \forall m, \text{ and } \left| \sum s_m \right| \leq s_{\text{max}}. \quad (9)$$

As the numerical evaluations will show, the resulting electric fields are more focal than those produced by (8), but at the expense of larger current flow through the brain. In addition, the resulting current distributions are more broadly distributed than with the  $\ell_1$  norm constraint.

### B. Optimizing for Intensity

The optimization of focality corresponds to maximizing tDCS safety, as undesired brain regions are spared by the stimulation. In some cases, it may be desirable to sacrifice focality and rather maximize the electric field at the target location. The framework of (4) easily allows one to formulate the problem of optimizing intensity: recall from (5) that  $\mathbf{C}$  consists of the rows of  $\mathbf{A}$  corresponding to the target node, while  $\mathbf{e}_o$  denotes the desired field orientation at the target. Thus, the maximization of the intensity in the desired direction at the target takes the form of a linear programming problem:

$$\begin{aligned} \mathbf{s}_{\text{max}} = \arg \max_{\mathbf{s}} \mathbf{e}_o^T \mathbf{C}\mathbf{s} \text{ subject to:} \\ \sum |s_m| + \left| \sum s_m \right| \leq 2s_{\text{max}}, \end{aligned} \quad (10)$$

where it should be noted that  $\mathbf{e}_o^T \mathbf{C}\mathbf{s}$  is the projection of the electric field at the target node on a vector pointing in the direction of the desired field.

## IV. PERFORMANCE METRICS

In order to assess the focality of a given field, we define the following metric which quantifies the proportion of the electric field magnitude contained within a sphere of increasing radius around the target:

$$\mathcal{F}(r) = \frac{\sum_{n \in \mathcal{T}(r)} \|\mathbf{e}(\mathbf{r}_n)\|}{\sum_n \|\mathbf{e}(\mathbf{r}_n)\|}, \quad (11)$$

where  $\mathcal{T}(r)$  is a set consisting of all nodes within radius  $r$  of the target node. We define the ‘‘half-max-radius’’ (analogous to the full-width-half-max) as the radius which contains half of the total electric field:

$$r_{0.5} \triangleq r | \mathcal{F}(r) = 0.5. \quad (12)$$

An example for  $\mathcal{F}(r)$  and  $r_{0.5}$  is given in Figure 2. In the forthcoming results, we plot the half-max radius against the target intensity in the desired direction (i.e., the projection of the electric field at the target onto a unit vector pointing in the specified orientation).

The results will be compared to conventional large pad-electrodes. A pad-electrode is simulated, or sampled, as a square arrangement of 5 small electrodes (approximately 5 cm side-length; see Figures 4 and 5). To evaluate the relative

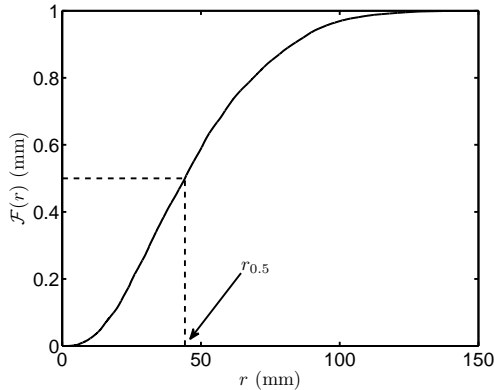


Fig. 2. Proportion of electric field confined in a sphere of increasing radius.

merits of optimization over the use of small electrodes, we also compare to current ad-hoc approaches for placing electrodes to achieve desired tangential and radial current directions. When specifying tangential current flow, the optimized results are compared to a bipolar configuration in which adjacent electrodes are oriented in the desired direction. In the case of a radial desired field, the benchmark will be the “4-by-1” configuration [16], in which the stimulating electrode is surrounded by 4 returns. For the sake of clarity, we refer to these benchmark configurations as “ad-hoc”.

## V. METHODS

The anatomical model was derived from an MRI of the head of a 35-year old healthy male recorded with a 3T Philips Achieva scanner (Philips Medical Systems, Amsterdam, Netherlands). The acquisition matrix has size 256-by-256-by-190 with a voxel size of 1mm-by-1mm-by-1mm. The image is then automatically segmented into four tissue categories (brain, CSF, scalp, and skull) using FSL’s Brain Extraction Tool and Automated Segmentation Toolbox (FSL, Oxford, UK). The model is then fitted with electrodes placed on the scalp according to the international 10/10 system; each electrode is modeled as a cylinder of 12mm diameter and 2mm depth. Additionally, conducting gel with a 1mm thick layer and surface area equal to that of the cylinder rests directly under the electrode. Manual correction of the automated segmentation is then performed using Simpleware’s ScanIP tool (Simpleware, Exeter, UK), followed by further segmentation of the volume into the following categories: electrode, conducting gel, brain, CSF, skull, scalp, air, and muscle. The segmented head is shown in Fig. 1. The labeled volume is then translated to a finite element mesh using Simpleware’s ScanFE software and isotropic conductivity values are assigned to each tissue type following Table I.

Laplace’s equation (1) is solved in Abaqus (Simulia, Providence, RI) by fixing one electrode as the reference (i.e., Cz), grounding the chosen reference, and then stimulating a single electrode with an input current density of 1 A/mm<sup>2</sup>; it was assumed that the current density is uniform across the surface of the electrode. This procedure is repeated for all

$M = 63$  free electrodes to yield the mixing matrix  $\mathbf{A}$ . Following this computation, the solutions were algebraically re-referenced to Iz which serves as the reference in the presented results. Finally, the optimization of currents was performed in MATLAB (Mathworks, Natick, MA) using disciplined convex programming [19]. In all cases, only the nodes corresponding to the brain were taken into account for the optimization.

## VI. RESULTS

To quantify the benefits of optimizing the applied currents and to establish an upper bound on achievable intensity and focality, we choose a cortical target for which we specify both radial and tangential stimulation (Fig. 3). We then compute the half-max radii and feasible target intensities for the following: simulated large-pad electrodes, two “ad-hoc” small electrode arrangements (4-by-1 or bipolar), and small-electrode arrays optimized for focality with the  $\ell_1$  norm constraint (8), optimized for focality with the individual electrode constraint (9), optimized for focality without safety constraint (7), and optimized for intensity (10). Figures 4a and 5a depict the focality-intensity curves for the radial and tangential directions, respectively. Additionally, we show the coronal slice of the electric fields and optimal current distributions for all six schemes in Figures 4b-g (radial) and 5b-g (tangential) – for all focality optimized schemes, the coronal slices are shown for a target intensity of 0.16 V/m (0.23 V/m) in the radial (tangential) case. The current distributions are displayed using a modified version of the EEGLAB topoplot function which renders the scalp currents in 2D [20] using the conventional schematic for the 10/10 international system <sup>2</sup>.

### Radial stimulation

Beginning with the radial case, note that with the simulated pad montage, the field intensity at the target is 0.16 V/m with a half-max radius of 80mm. Meanwhile, the ad-hoc 4-by-1 configuration attains the same target intensity with an  $r_{0.5}$  of 57mm. Immediately, the benefits of optimizing for focality become apparent, as the LCMV- $\ell_1$  scheme achieves field intensities of up to 0.25 V/m (the curve terminates at the maximum feasible intensity, while maintaining a half-max radius less than 69mm. At the intensity attained by the simulated pad and ad-hoc schemes (0.16 V/m), the LCMV- $\ell_1$  method yields an 80% improvement in focality over the pads and 47% over the ad-hoc scheme. <sup>3</sup>

As expected due to the increased degrees of freedom, the LCMV with currents constrained at each electrode exhibits an excellent focality-intensity trade-off:  $r_{0.5}$  of 40mm at 0.3 V/m. Most striking is the fact that the the LCMV method with unconstrained currents achieves a half-max radius of only 30mm – note that only the magnitude, and not the distribution of the optimal unconstrained currents (7) change with an

<sup>2</sup>The coronal slice is shown using the radiological convention: from the vantage point of the clinician facing the patient. Note that the visualization of the scalp currents is thus flipped left-to-right with respect to the slice.

<sup>3</sup>We define the improvement as the percentage decrease in the volume containing half of the electric field ( $\propto r_{0.5}^3$ ).

increased target intensity; thus,  $r_{0.5}$  remains constant. Turning to Figure 4f, we observe that this unconstrained solution resembles a “spherical sinc” function, with rings of alternating polarity centered over the target.

It is interesting to note that the LCMV- $\ell_1$  solution (Figure 4d) is a non-trivially modified version of the ad-hoc 4-by-1, with the difference being the location and magnitude of the return electrodes. This slight difference accounts for a significant reduction in half-max radius. Herein lie the benefits of performing a patient-specific optimization of the applied currents: the nominal 4-by-1 arrangement is only an approximation to the ideal solution (the unconstrained LCMV), and the idiosyncrasies of patient anatomy are indispensable to the computation of the maximally focal configuration (i.e., which electrodes to use as the returns, and how much current to pass through them).

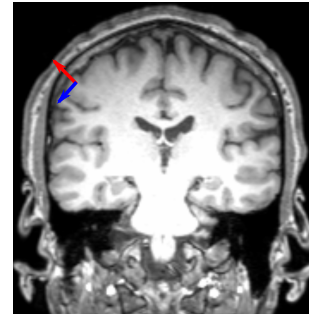
Finally, the maximum intensity scheme yields a target intensity of 0.31 V/m, representing a 97% (98%) improvement in achieved target intensity over the simulated pad (ad-hoc 4-by-1) montage, while using the same amount of input current. From Figure 4g, the intensity optimized configuration takes the form of a “semi-distant” bipolar, with the stimulating electrode placed directly over the target. The optimization scheme here serves to identify the placement of the most intense bipolar configuration.

#### *Tangential stimulation*

Consider now Figure 5a, which details the focality-intensity trade-off in the case of tangential stimulation. In this case, the simulated pad and ad-hoc bipolar montages attain target intensities of 0.23 and 0.29 V/m and half-max radii 80 and 69mm, respectively. At 0.23 V/m, the  $\ell_1$  norm constrained solution yields an improvement of 52% in focality over the simulated pad scheme. Moreover, the improvement over the ad-hoc bipolar montage at 0.29 V/m is 12%. The reduced improvement in focality compared to the radial case may be attributed to the fact that tangential stimulation leads to larger target intensities – at these larger intensities, there are fewer degrees of freedom available to the optimization schemes.

The individually constrained and unconstrained LCMV solutions yield massive improvements over conventional methods, with the half-max radius not exceeding 45mm at 0.29 V/m. Note that the unconstrained currents resemble a spherical sinc with non-arbitrary weights applied to the involved electrodes and an additional ring emerging (compared to the radial case). It is difficult to find structure in the individually constrained optimal current configuration.

In terms of target intensity, the maximum intensity scheme yields a target intensity of 0.48 V/m, representing an improvement of 63% and 112%, respectively, over the simulated pad and ad-hoc bipolar montages. The maximally intense montage is bipolar with the pair of electrodes arranged in the direction of desired orientation, and the target resting between the electrodes. Here again, the optimization’s role is not in determining amount of current injected, but rather the location of the bipolar montage.



(a) Target

Fig. 3. Targeting a cortical node in radial (red) and tangential (blue) directions.

## VII. DISCUSSION

We have demonstrated that the nature of the safety criteria drastically affects the resulting optimal solutions. The more conservative safety criterion of limiting the total current had the advantage of leading to solutions with a small number of electrodes. It may also be useful to modify the proposed approach and explicitly search for the best subset of electrode locations among a large number of candidate locations (e.g., 5 out of 64, if 4 is the available number of independently controlled stimulators).

At present, many clinical trials have no well-defined target areas; until further clarity emerges on the desired target locations for specific conditions, it may be that focal stimulation is not desirable: if the target is unknown, one may stimulate broadly and rely on the behavioral paradigm for specificity. However, if efficacy and safety are to be systematically optimized, we believe that it is paramount to identify the precise site of action of electrical stimulation paradigms – in that case, the present results justify the increased complexity in software and hardware required for targeting.

Experimental work is still outstanding to establish the importance of stimulation orientation. Radial and tangential directions were defined here relative to the skull as this surface is the major determinant for placing electrodes. From a functional point of view, the target direction will likely be defined based on the cortical anatomy, which due to its extensive folding, does not necessarily correspond to the tangential or radial directions defined here.

The customarily employed distant bi-polar configuration may be optimal in terms of intensity (at least in the case of a radial target), but certainly not focality. Despite its simplicity, the ad-hoc bipolar configuration considered in this paper is not currently used in practice. We have found that this configuration is a reasonable approximation to the optimal configuration in the case of a desired tangential field. While in hindsight the solution seems obvious, the dependence of electrode configuration on desired field orientation has so far not been recognized. For example, the 4-by-1 montage is a suitable design for radially oriented currents, but is unlikely to be appropriate for tangential fields.

Another finding which is intuitively satisfying relates to

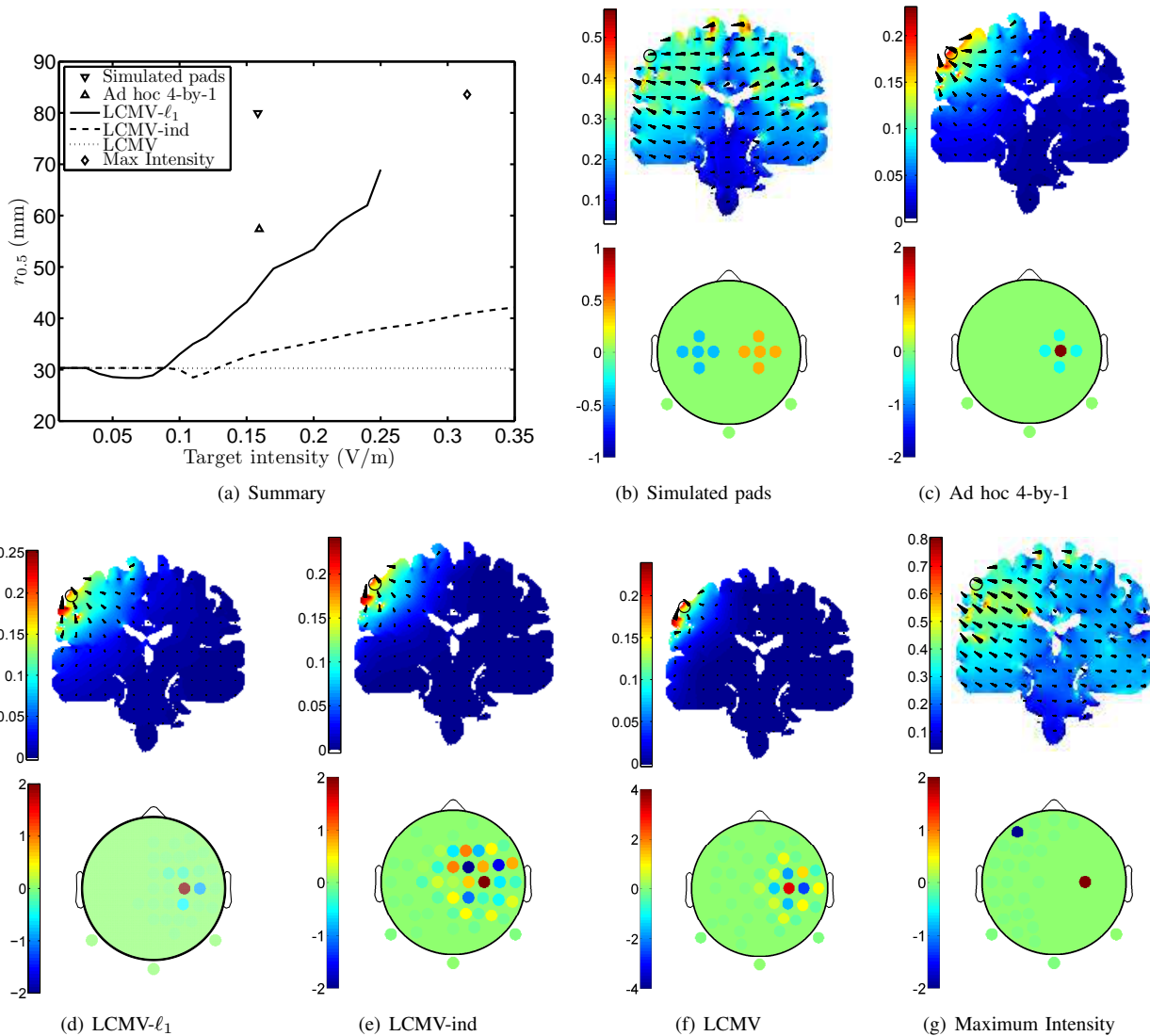


Fig. 4. Focality-intensity trade-off and the algorithms that balance them: radial desired field. In (d)–(f), electric field slices and optimal current distributions are shown for a target intensity of 0.16 V/m.

the location of the maximally intense bipolar configuration. In the case of tangential stimulation, naive placement of large electrodes over the target region misses the point of maximal stimulation which lies between electrodes and not directly under the pad. On the other hand, when desiring radial stimulation, the stimulating electrode is indeed best placed above the target, with the return electrode positioned at a disparate altitude.

## VIII. CONCLUSION

This paper has presented a novel, multi-electrode paradigm for non-invasive electrical stimulation in which a patient-specific MRI-based model of the head is utilized to determine the electrode positions and current intensities which optimize the induced electric field in either focality or intensity. It was shown that the optimal stimulation parameters are strongly affected by both the desired field orientation at the target and

the optimization criterion (focality or intensity). Moreover, achievable focality is limited by the safety constraint on maximum currents. To maximize target field intensity under an  $\ell_1$  safety constraint, the optimal configuration is bipolar with ample separation between anode and cathode. The results indicate that both focality as well as intensity at the target can be drastically improved over the conventional approach of using large pad-electrodes.

## REFERENCES

- [1] M. A. Nitsche and W. Paulus, "Excitability changes induced in the human motor cortex by weak transcranial direct current stimulation," *Journal of Physiology*, 527.3, pp. 633–639, 2000.
- [2] P. S. Boggio et al., "Go-no-go task performance improvement after anodal transcranial DC stimulation of the left dorsolateral prefrontal cortex in major depression." *J. Affect. Disord.* vol. 101, pp. 9198, 2007.
- [3] F. Fregni, S. Thome-Souza, M. A. Nitsche, S. D. Freedman, K. D. Valente, A. Pascual-Leone, "A controlled clinical trial of cathodal DC polarization in patients with refractory epilepsy." *Epilepsia*, vol. 47, pp. 335342, 2006.

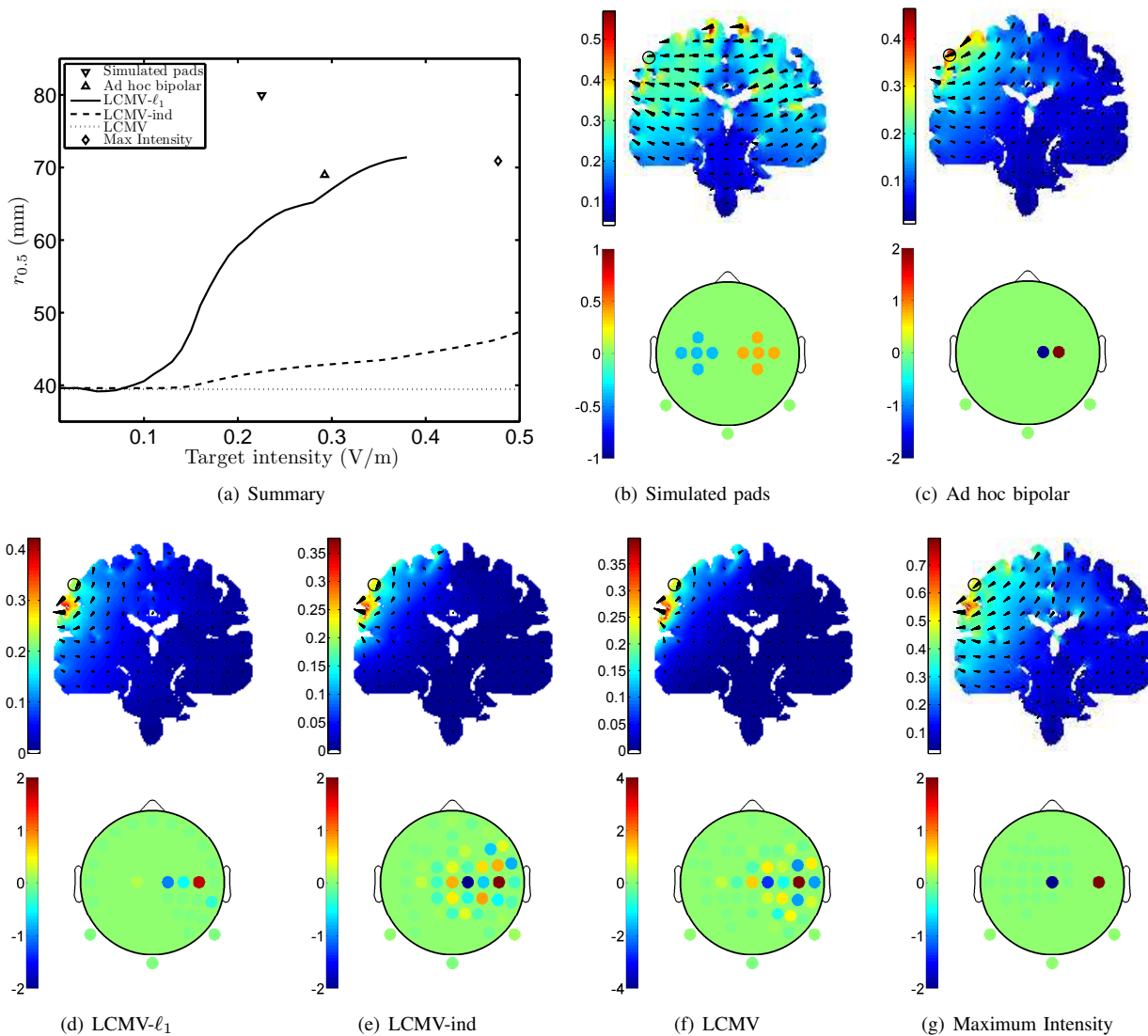


Fig. 5. Focality-intensity trade-off and the algorithms that balance them: tangential desired field. In (d)–(f), electric field slices and optimal current distributions are shown for a target intensity of 0.23 V/m.

[4] F. Fregni, D. K. Simon, A. Wu, A. Pascual-Leone, "Non-invasive brain stimulation for Parkinson's disease: a systematic review and meta-analysis of the literature." *J. Neurol. Neurosurg. Psychiatry*, vol. 76, pp. 1614-1623, 2005.

[5] F. Hummel et al., "Effects of non-invasive cortical stimulation on skilled motor function in chronic stroke." *Brain*, vol. 128, pp. 490-499, 2005.

[6] J. M. Baker, C. Rorden, J. Fridriksson, "Using transcranial direct-current stimulation to treat stroke patients with aphasia." *Stroke*, vol. 41, no. 6, pp. 1229-36, 2010.

[7] F. Fregni, P. S. Boggio, M. A. Nitsche, F. Bormpohl, A. Antal, E. Feredoes, et al., 2005a. Anodal transcranial direct current stimulation of prefrontal cortex enhances working memory. *Exp. Brain Res.* 166, 2330.

[8] M. B. Iyer, U. Mattu, J. Grafman, M. Lomarev, S. Sato, E. M. Wassermann, "Safety and cognitive effect of frontal DC brain polarization in healthy individuals." *Neurology*, vol. 64, pp. 872-875, 2005.

[9] P. C. Miranda, M. Lomarev, and M. Hallett, "Modeling the current distribution during transcranial direct current stimulation," *Clinical Neurophysiology*, 117, pp. 1623-1629, 2006.

[10] R. N. Holdefer, R. Sadleir, and M. J. Russell, "Predicted current densities in the brain during transcranial electrical stimulation," *Clinical Neurophysiology*, 117, pp. 1388-1397, 2006.

[11] T. Wagner, F. Fregni, S. Fecteau, A. Grodzinsky, M. Zahn, and A. Pascual-Leone, "Transcranial direct current stimulation: a computer-based human model study," *NeuroImage*, vol. 35, pp. 1113-1124, 2007.

[12] C. W. Im, H. H. Jung, J. D. Choi, S. Y. Lee, and K. Y. Jung, "Determination of optimal electrode positions for transcranial direct current stimulation," *Physics in Medicine and Biology*, 53, pp. N219-N225, 2008.

[13] H. S. Suh, W. H. Lee, Y. S. Cho, J. H. Kim, and T. S. Kim, "Reduced spatial focality of electrical field in tDCS with ring electrodes due to tissue anisotropy." in *Proc. IEEE Eng. Med. Biol. Soc.*, vol. 1, pp. 2053-2056, 2010.

[14] J. H. Park, D. W. Kim, and C. H. Im, "A novel array-type transcranial direct current stimulation (tDCS) system for accurate focusing on targeted brain regions." in *Proc. Biennial IEEE Conference on Electromagnetic Field Computation*, 2010.

[15] D. Griffiths, *Introduction to Electrodynamics*, Prentice-Hall: Upper Saddle River, NJ, 1999.

[16] A. Datta, V. Bansal, J. Diaz, J. Patel, D. Reato, M. Bikson, "Gyri-precise head model of transcranial DC stimulation: Improved spatial focality using a ring electrode versus conventional rectangular pad." *Brain Stimulation*, vol. 2(4), pp. 201-207, 2009.

[17] D. Logan, *A First Course in the Finite Element Method*. Nelson: Toronto, 2007.

[18] B. D. Van Veen and K. M. Buckley, "Beamforming: a versatile approach to spatial filtering." *IEEE ASSP Magazine*, vol. 5, pp. 4-24, 1998.

[19] M. Grant, S. Boyd, and Y. Ye, "Disciplined Convex Programming." Chapter in *Global Optimization: From Theory to Implementation*, L. Liberti and N. Maculan (eds.), Springer, pages 155-210, 2006.

[20] A. Delorme and S. Makeig, "EEGLAB: an open source toolbox for analysis of single-trial EEG dynamics." *Journal of Neuroscience Methods*, vol. 134, pp. 9-21, 2004.